SUPPLEMENTARY INFORMATION
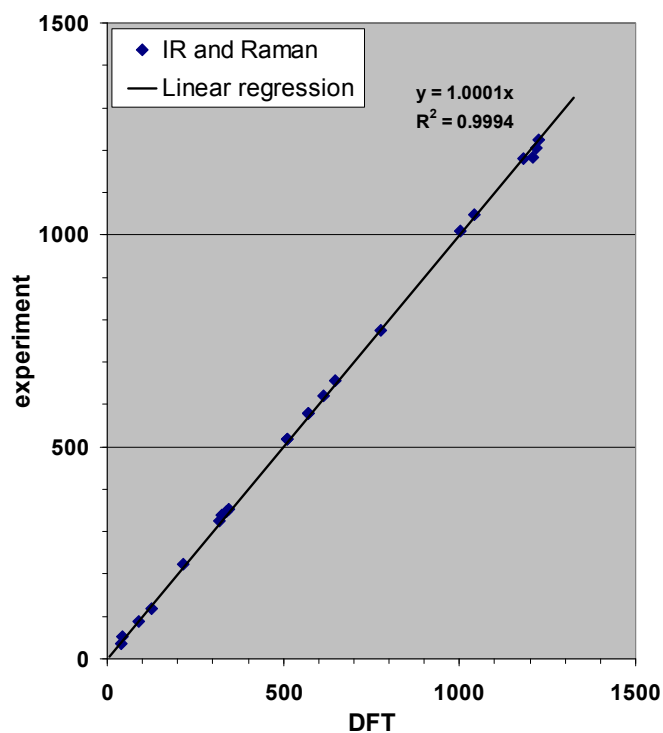
Crystal and electronic structure, lattice dynamics and thermal properties of Ag(I)(SO$_3$)R (R=F, CF$_3$) Lewis acids in the solid state

Wojciech Grochala, Michał Ksawery Cyrański, Mariana Derzsi, Tomasz Michałowski,

Przemysław J. Malinowski, Zoran Mazej, Dominik Kurzydłowski, Wiktor Koźmiński,

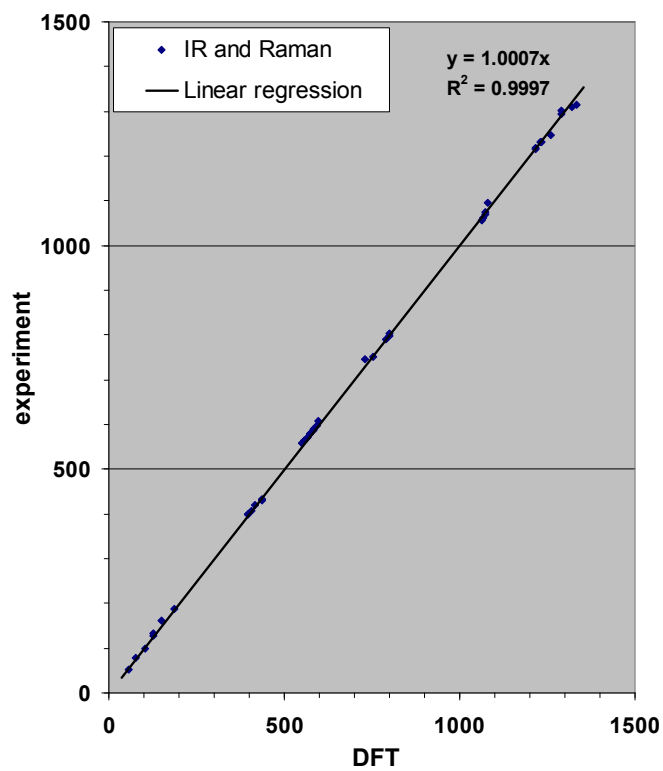Armand Budzianowski, and Piotr J. Leszczyński

Contents

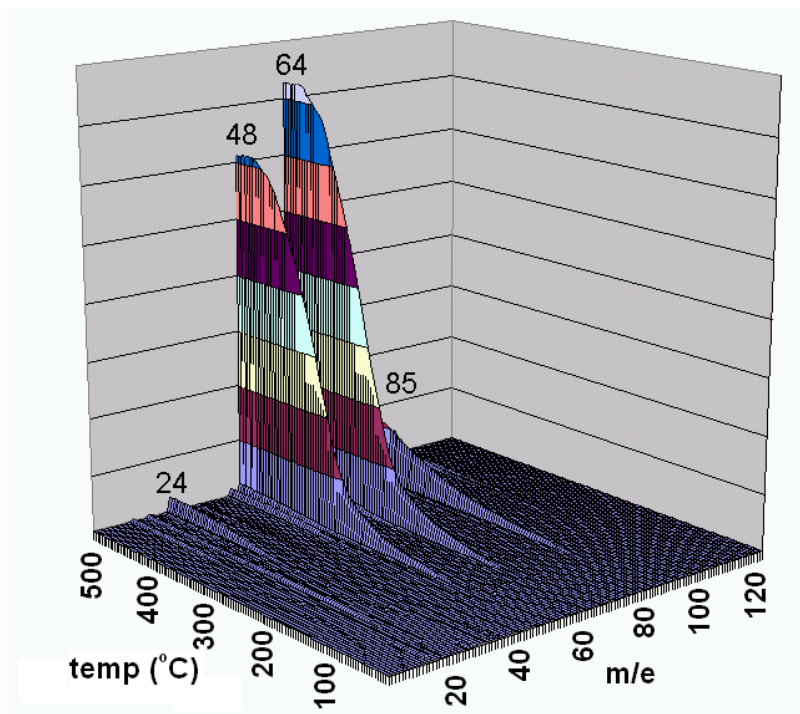**S1. Correlation between theoretical and experimental values of wavenumbers [cm⁻¹] for phonon modes of AgSO₃CF₃.**

S2. Correlation between theoretical and experimental values of wavenumbers [cm⁻¹] for phonon modes of AgSO₃F.

S3. The EGA data for thermal decomposition of AgSO₃F.

S4. The IR spectrum and XRDP of solid residue obtained during thermal decomposition of AgSO₃F at 500 °C.
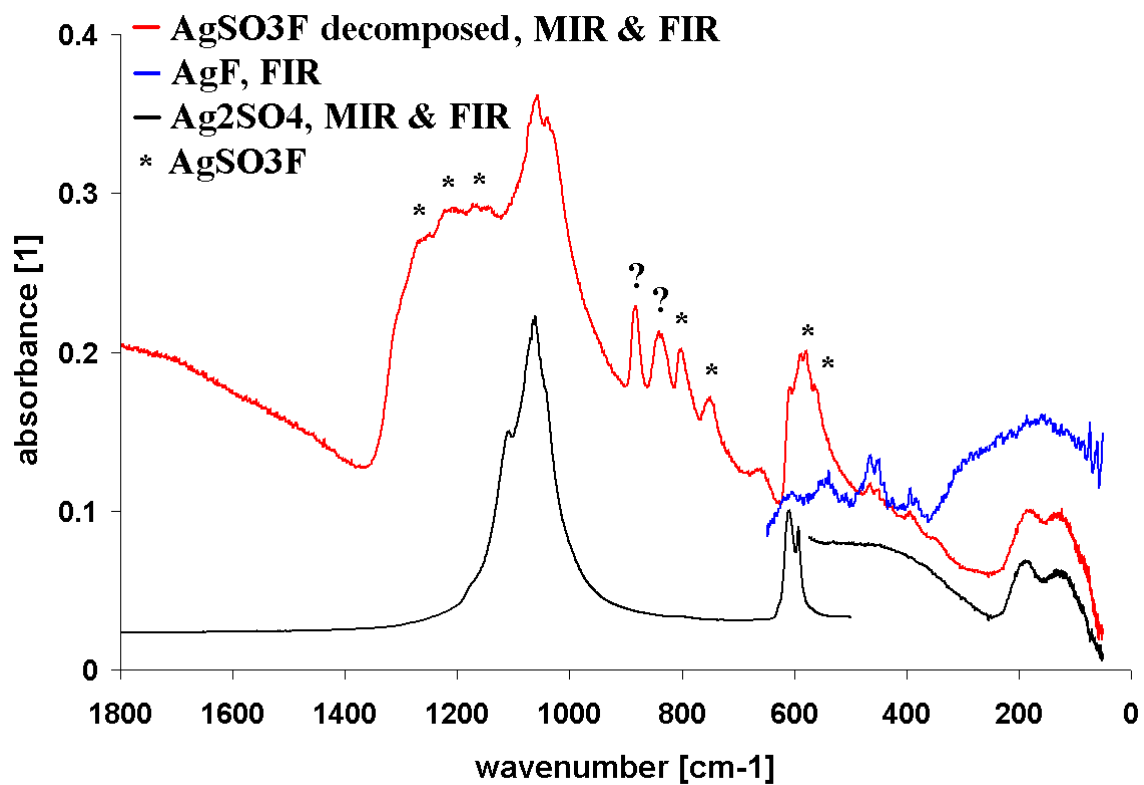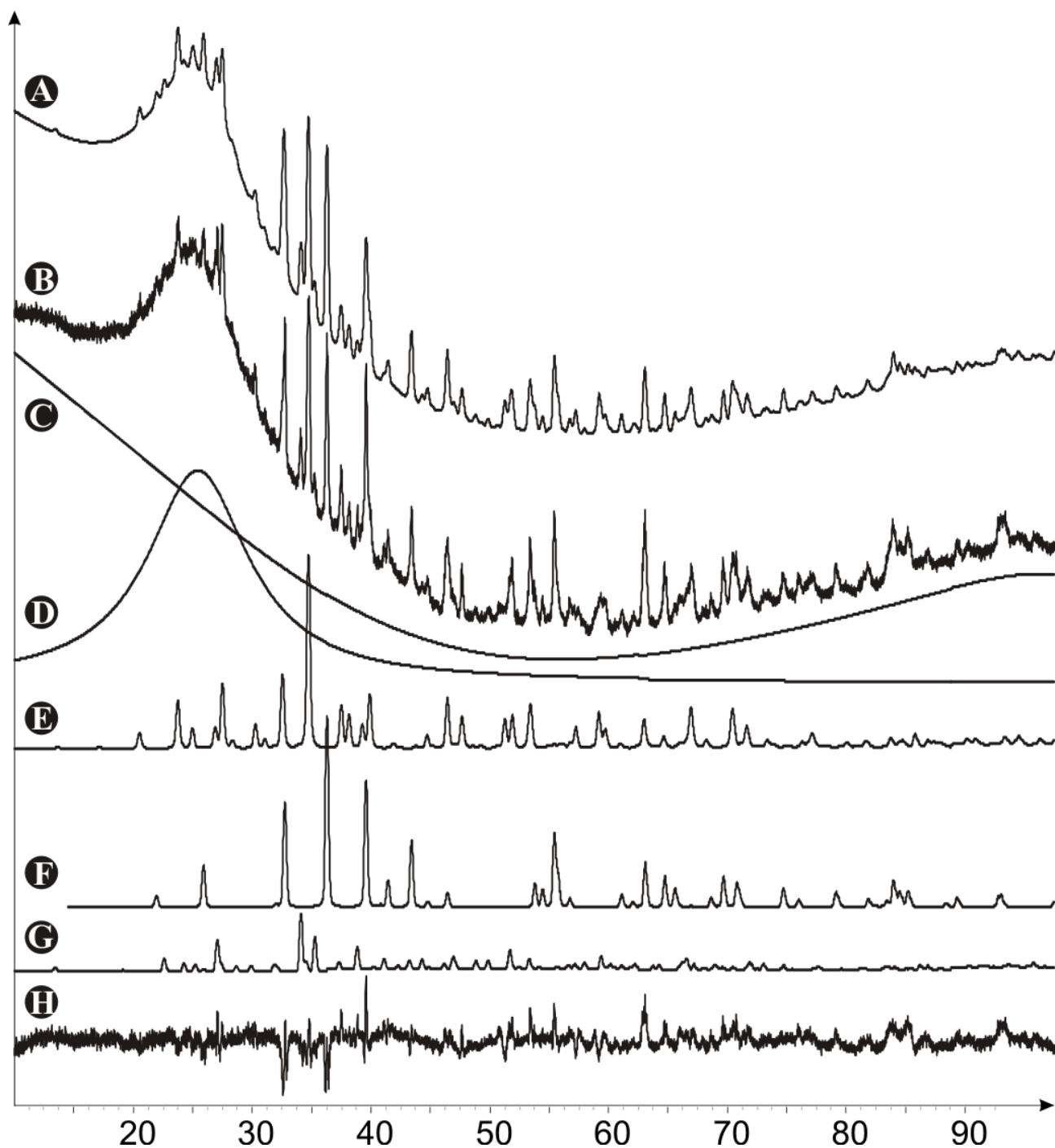
A – the calculated XRD pattern, B – the measured XRD pattern; C – background; D – amorphous hump (capillary); E – $AgHSO_4$ ($P2_1/c$)*; F – Ag_2SO_4 (Fddd); G – residual $AgSO_3F$ ($P2_1/m$); H – differential pattern B-(C+D+E+F+G).

- **IMPORTANT!** Presence of $AgHSO_4$ suggests that its anhydrous precursor, $Ag_2S_2O_7$, was present in the thermally decomposed samples, and it reacted instantly with moisture during a very short exposure of the samples to atmosphere during their transfer from TGA-DSC apparatus to the glovebox.

S5. The EGA data for thermal decomposition of AgSO₃CF₃.

-
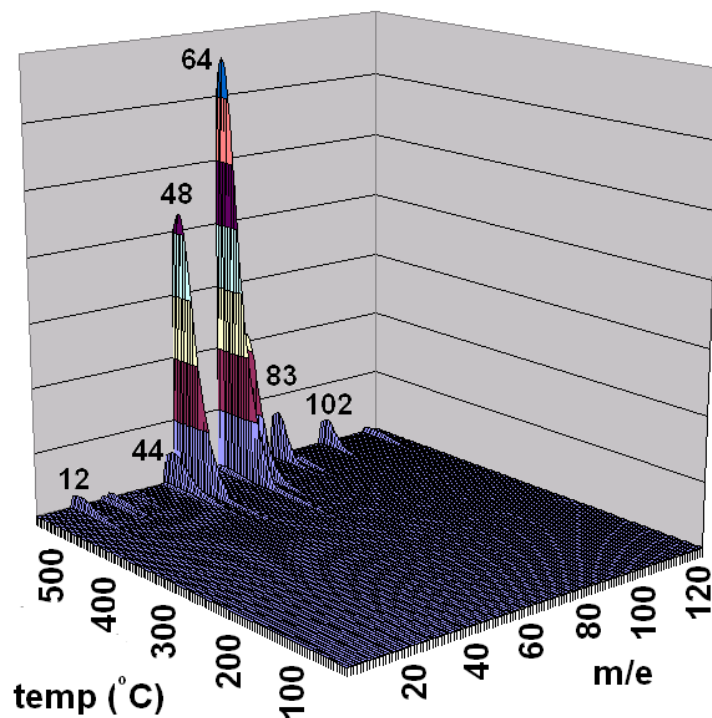

S6. The IR spectrum and XRDP of solid residue obtained during thermal decomposition of AgSO₃CF₃ at 500 °C.
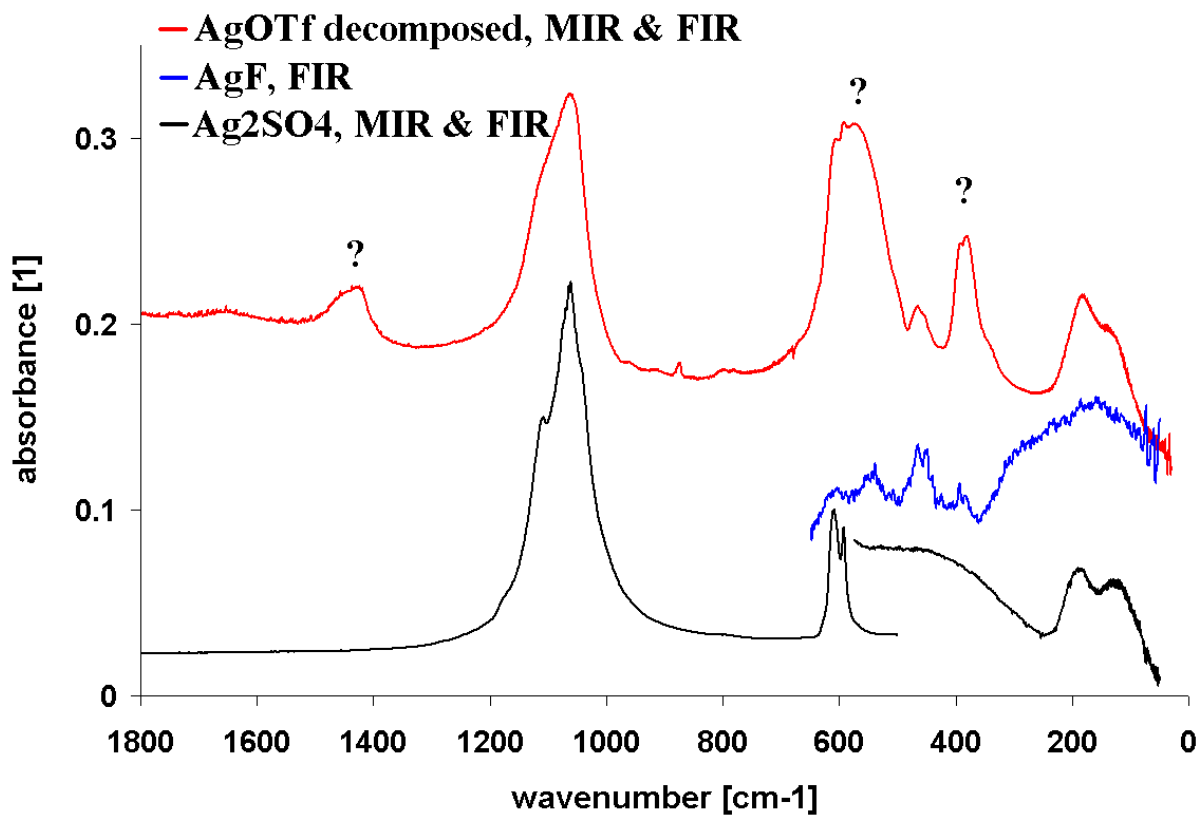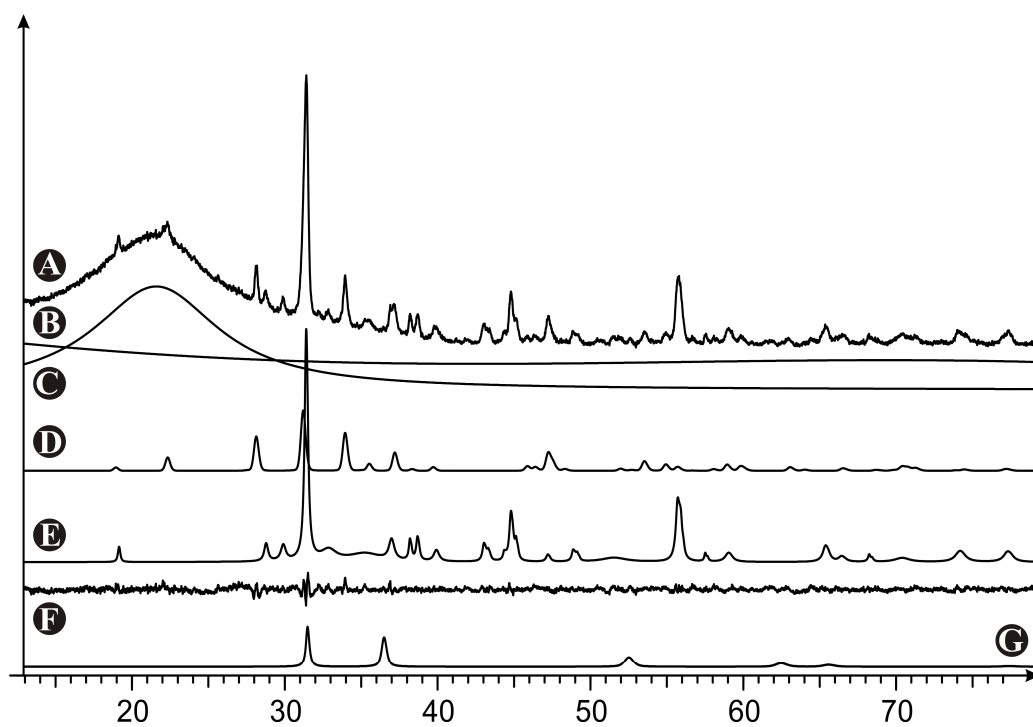
A – the measured XRD pattern; B – background; C – amorphous hump (capillary); D - Ag_2SO_4 (Fddd);
E – the pattern coming from the remaining reflexes (see below); F – differential pattern A-(B+C+D+E);
G – theoretical pattern for AgF (Fm-3m) to emphasize absence of two important reflections.

S7. The XRD patterns of AgSO₃CF₃ at RT, 260 °C, 310 °C, 350 °C, and again at RT, and lattice constants obtained from Pawley fits.
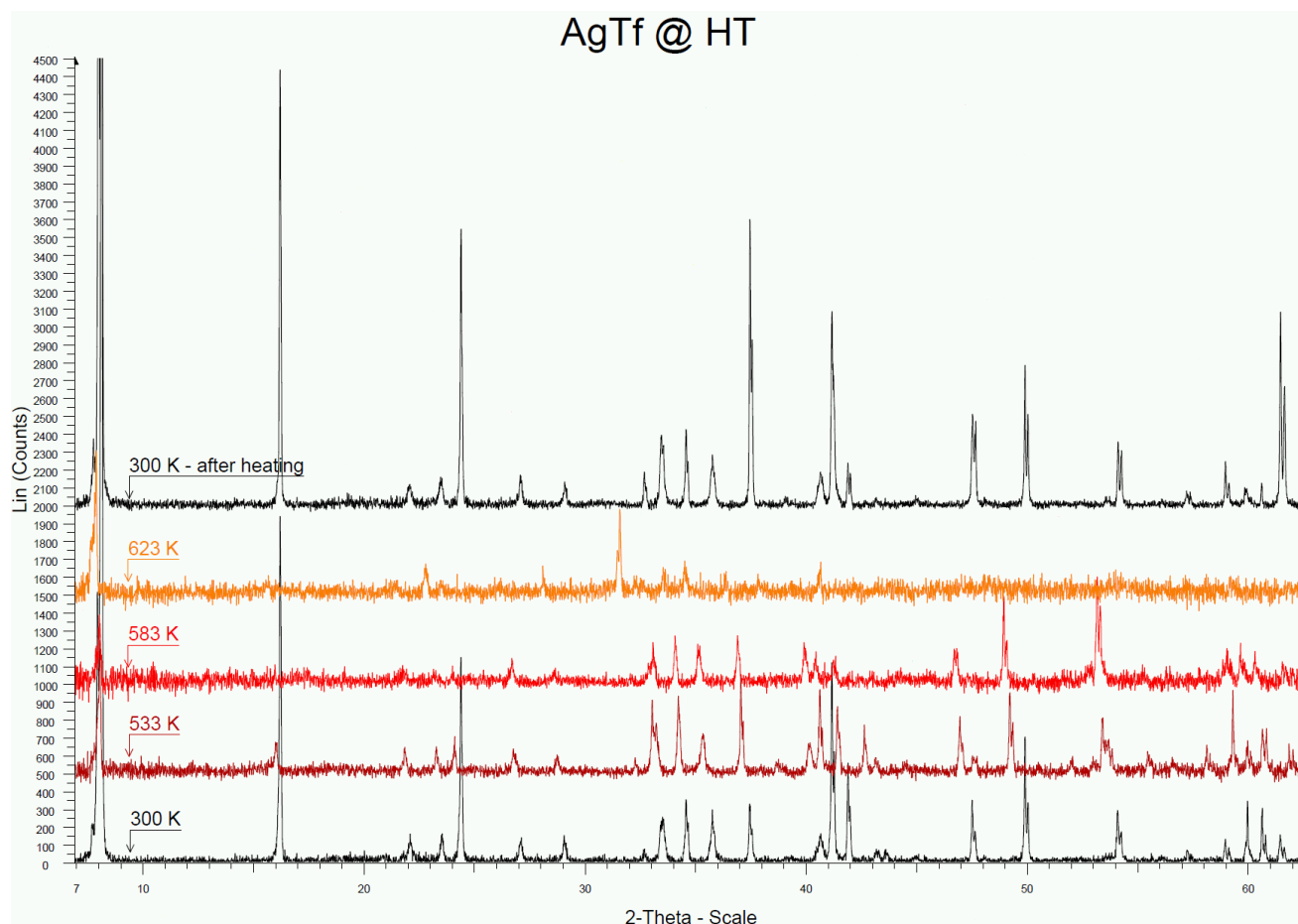
The high-T XRD patterns of AgOTf resemble those of the low-T phase except for dramatic changes of intensities for selected reflections (notably 003, 006 and 009), likely due to free rotation of CF_3 and SO_3 groups and/or increased mobility of Ag^+ cations. All patterns can be indexed using hexagonal cell (**Table S7**).

Table S7 The hexagonal cell lattice vectors (a, c) and unit cell volume (V) for $AgSO_3CF_3$ at various temperatures.

T /K	a /Å	c /Å	V /Å³
100[a]	5.312(3)	32.66(2)	798.1(8)
300[b]	5.3290(5)	32.812(3)	806.96(14)
533[c]	5.392(1)	33.302(1)	838.63(6)
583[c]	5.413(1)	33.462(3)	849.23(16)
623[c]	5.488(3)	33.960(17)	885.67(98)

[a] *Single crystal data;* [b] *Rietveld fit, powder data;*
[c] *Pawley fit, powder data (the GOF varies between 1.11 and 1.17).*

S8. Analysis of the electronic band structure and DOS for AgSO₃R (R=F, CF₃) – DFT view

Just like majority of common oxo salts of Ag(I), AgSO₃R salts (R=F, CF₃) are colourless solids at ambient conditions. This indicates that their direct electronic bandgaps, Δ_F, at the Fermi level (E_F) exceed 3.1 eV (equivalent of 400 nm, *i.e.* a borderline between VIS and NUV regions of electromagnetic spectrum). To get insight into electronic structure of both title compounds we have carried out electronic band structure and density of state (DOS) calculations (**Figures S8.1 & S8.2**), and compared with results obtained for related Ag₂SO₄ (**Table S8**).

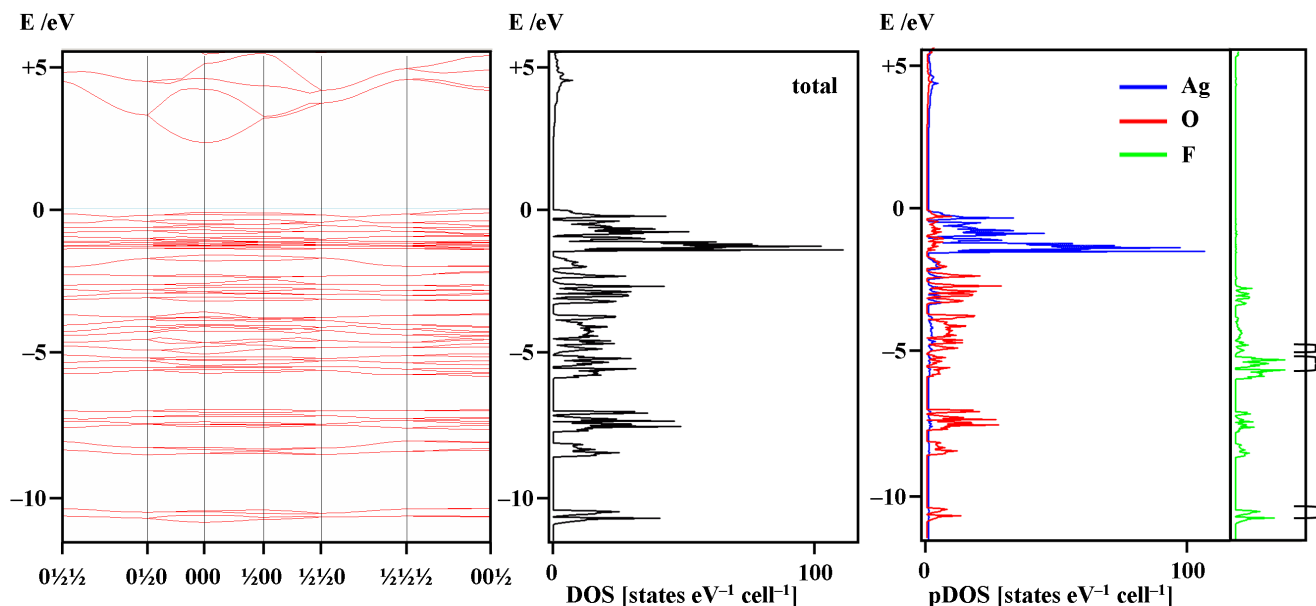### S8.1. Electronic structure of AgSO₃F.

Figure S8.1 The electronic band structure (left), the total density of states (DOS, middle) and the partial atomic densities of states (pDOS, right) for AgSO₃F; the PBEsol results (VASP); Z=4. The Fermi level was set to zero.

The electronic band structure of AgSO₃F (Z=4) exhibits many rather flat occupied bands and as such it is typical for compounds of Ag(I) with large spatial separation between Ag(I) cations. The Ag(d) states predominate DOS in the –1.5 eV to 0.0 eV energy range forming a rather large DOS peak with a maximum close to –1.4 eV. Ligand states mix only very weakly with the metal states, confirming ionic character of metal–ligand bonding. The uppermost 8 bands form the e_g set (metal–ligand antibonding σ* states) and the bottom 12 bands the t_{2g} set (metal–ligand antibonding π*). Below them one finds 32 bands in the –3.3 eV to –8.5 eV energy range; the uppermost 12 can be assigned to metal-ligand non-bonding orbitals (mostly 'lone pairs' on O atoms of SO₃F⁻ anions), while the bottom 20 to the metal–ligand bonding π and σ states. The eight bands –7.6 eV and –6.9 eV have large contribution from S (not shown) and they correspond to S–O bonding orbitals. The four bands between –8.5 eV and –8.0 eV originate mostly from the lone pairs on F atoms, while the four between –10.8 eV and –10.3 eV from the S–F bonding σ states.

The calculated direct band gap at the Fermi level of only 2.4 eV (at the center of Brillouin zone) is certainly underestimated, as typical for DFT methods. The broad conduction band is mostly of the Ag(4s) origin, as for majority of compounds of Ag(I).

S8.2. Electronic structure of AgSO₃CF₃.

The electronic band structure of AgOTf (Z=2) is in one way similar to that of $AgSO_3F$ – most occupied bands are rather flat. However, some of the bands originating from metal–ligand antibonding orbitals have larger dispersion (up to 0.5 eV) in comparison to those found for $AgSO_3F$. The reason for that is in short Ag…Ag separation and in 2D character of the crystal lattice of AgOTf. Due to this larger dispersion, there is no clear gap between the metal–ligand antibonding states (formally 10 of them down to −1.9 eV below E_F) and the non-bonding electrons on O atoms – even the 13th band below the Fermi level still contains substantial contribution from Ag atoms. Moreover, the e_g and t_{2g} sets are no longer well separated in the energy scale (as it takes place for $AgSO_3F$) which is due to strong d-d inter-orbital interaction at neighbouring Ag centers. In this energy range the O(2p) orbitals are somewhat more mixed up with Ag(4d) than it took place for $AgSO_3F$. Some of the lone pairs on F atoms are now found as close to the Fermi level as at −4 eV; this is due to repulsive lone-pair lone-pair interactions at CF_3 groups.
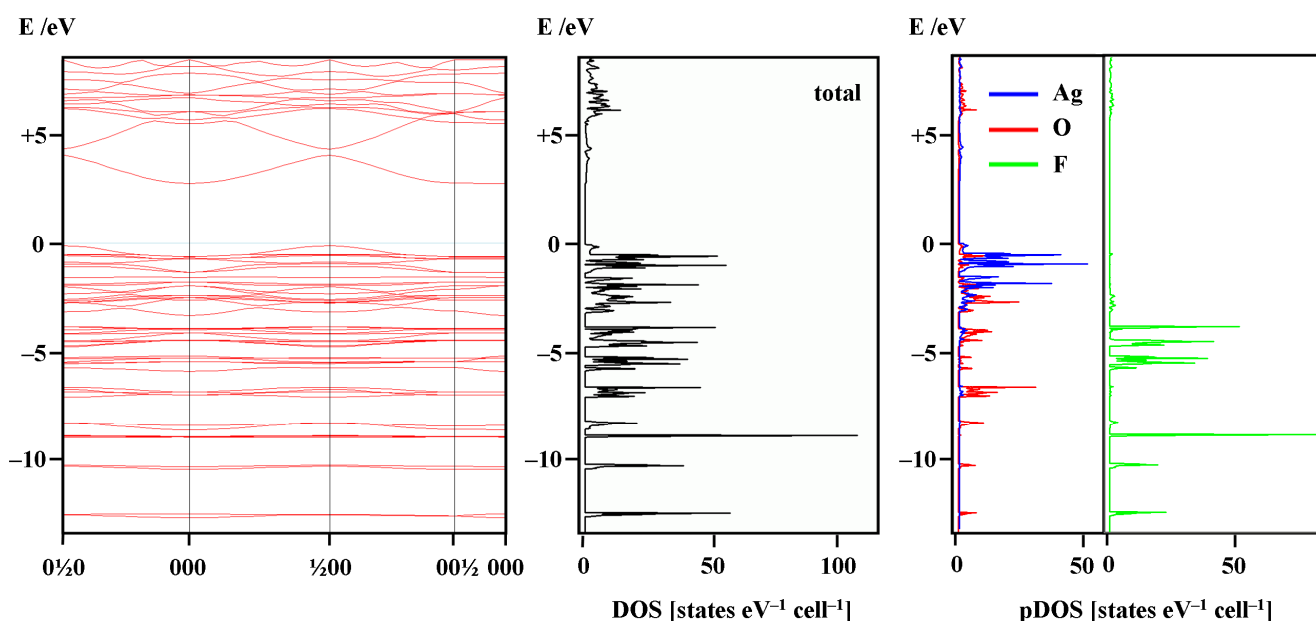

Figure S8.2 The electronic band structure (left), the total density of states (DOS, middle) and the partial atomic densities of states (pDOS, right) for $AgSO_3CF_3$; the PBEsol results (VASP); Z=4. The Fermi level was set to zero.

The calculated direct band gap of 3.4 eV (at the center of Brillouin zone) is by 1 eV larger than that calculated for $AgSO_3F$; this is due to the fact that CF_3 group is a better electron acceptor than a single F atom.[i] One finds an indirect band gap of 2.9 eV. The broad conduction band is again mostly of the Ag(4s) origin, as expected.

The calculated electron density distribution on metal cation and anion is similar for $AgSO_3CF_3$, $AgSO_3F$ and the related Ag_2SO_4 (Table S8), no matter whether the traditional Mulliken or rather Hirschfeld population analysis is applied; the Ag–O bond polarities are similar for these oxo compounds of Ag(I).

Table S8 The DFT-calculated Hirschfeld[ii] and Mulliken[iii] atomic charges for $AgSO_3R$ (R=F, CF_3) as compared to Ag_2SO_4 reference (CASTEP results).

Atom	Hirschfeld			Mulliken		
	Ag_2SO_4	$AgSO_3F$	$AgSO_3CF_3$	Ag_2SO_4	$AgSO_3F$	$AgSO_3CF_3$
Ag	+0.28	+0.30	+0.30	+0.55	+0.66	+0.61
O	−0.25	−0.23	−0.24	−0.84	−0.86	−0.86
S	+0.43	+0.47	+0.40	+2.28	+2.38	+2.13
F	---	−0.08	−0.06	---	−0.48	−0.32
C	---	---	+0.21	---	---	+0.81
$[SO_3]^a$	−0.32	−0.22	−0.32	−0.24	−0.20	−0.45
$[CF_3]^a$	---	---	+0.03	---	---	−0.15

^{a} *Charge on the functional group calculated from atomic charges.*

[i] See for example: B. T. King, J. Michl, *J. Am. Chem. Soc.* **122**, 10255-10256 (2000) and references therein.

[ii] F. L. Hirshfeld, *Theor. Chim. Acta* **44**, 129-138 (1977).

[iii] R. S. Mulliken, *J. Chem. Phys.* **23**, 1833-1831 (1955).